SUPPLEMENTARY INFORMATION

CRYPTIC GENOMIC LESIONS IN ADVERSE-RISK ACUTE MYELOID LEUKEMIA IDENTIFIED BY INTEGRATED WHOLE GENOME AND TRANSCRIPTOME SEQUENCING

Jaeseung C. Kim[1,2,3], Philip C. Zuzarte[2], Tracy Murphy[3], Michelle Chan-Seng-Yue[3,4], Andrew M. K. Brown[2], Paul M. Krzyzanowski[2], Adam C. Smith[5], Faiyaz Notta[1,3,4], Mark D. Minden[1,3], and John D. McPherson[1,2,6]

[1]Department of Medical Biophysics, Faculty of Medicine, University of Toronto, Toronto, ON, Canada;

[2]Genomics Technology Program, Ontario Institute for Cancer Research, Toronto, ON, Canada;

[3]Princess Margaret Cancer Centre, University Health Network, Toronto, ON, Canada;

[4]PanCuRx Translational Research Initiative, Ontario Institute for Cancer Research, Toronto, ON, Canada;

[5]Department of Laboratory Medicine and Pathobiology, University of Toronto and the Laboratory Medicine Program, University Health Network, Toronto, ON, Canada;

[6]Biochemistry and Molecular Medicine, University of California, Davis, Sacramento, CA, USA

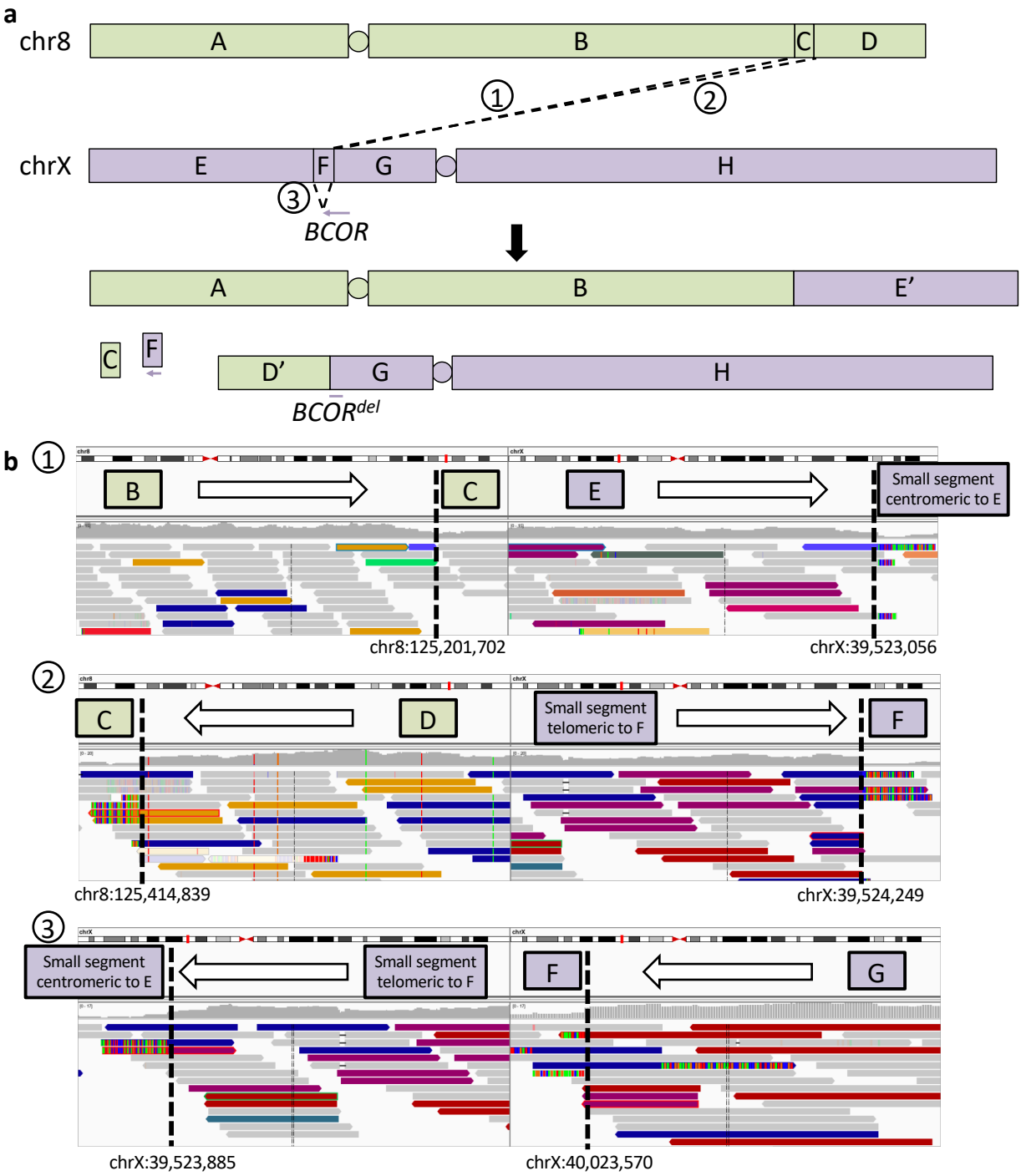

Supplementary Figure 1. Three SVs involved in t(X;8) and *BCOR* deletion in case 2. **a** Schematic representation of SVs as in Fig. 1 b, f. **b** Integrative Genomics Viewer (IGV) visualization of sequencing reads involved in each SVs. Boxes represent genomic segments, dashed lines represent breakpoints, and arrows represent directions of discordant Illumina paired-end reads. Orientations of rearranged genomic segments in **a** are inferred by re-orienting read pairs to point towards each other.

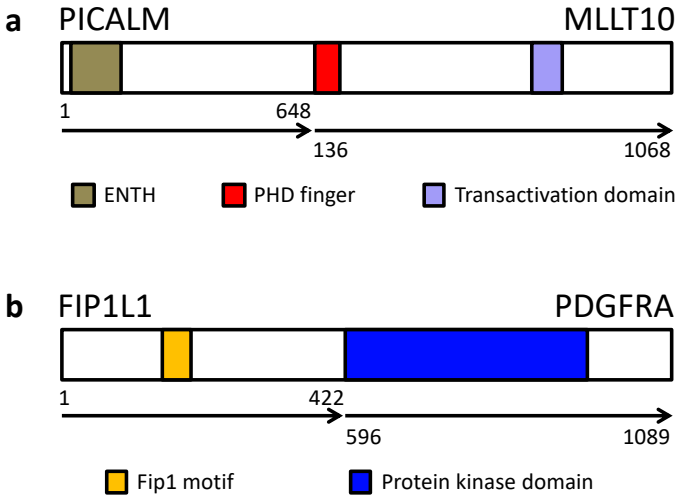

Supplementary Figure 2. Domain structures of **a** PICALM-MLLT10 and **b** FIP1L1-PDGFRA fusion proteins from case 5. See Fig. 1d, h for legends.

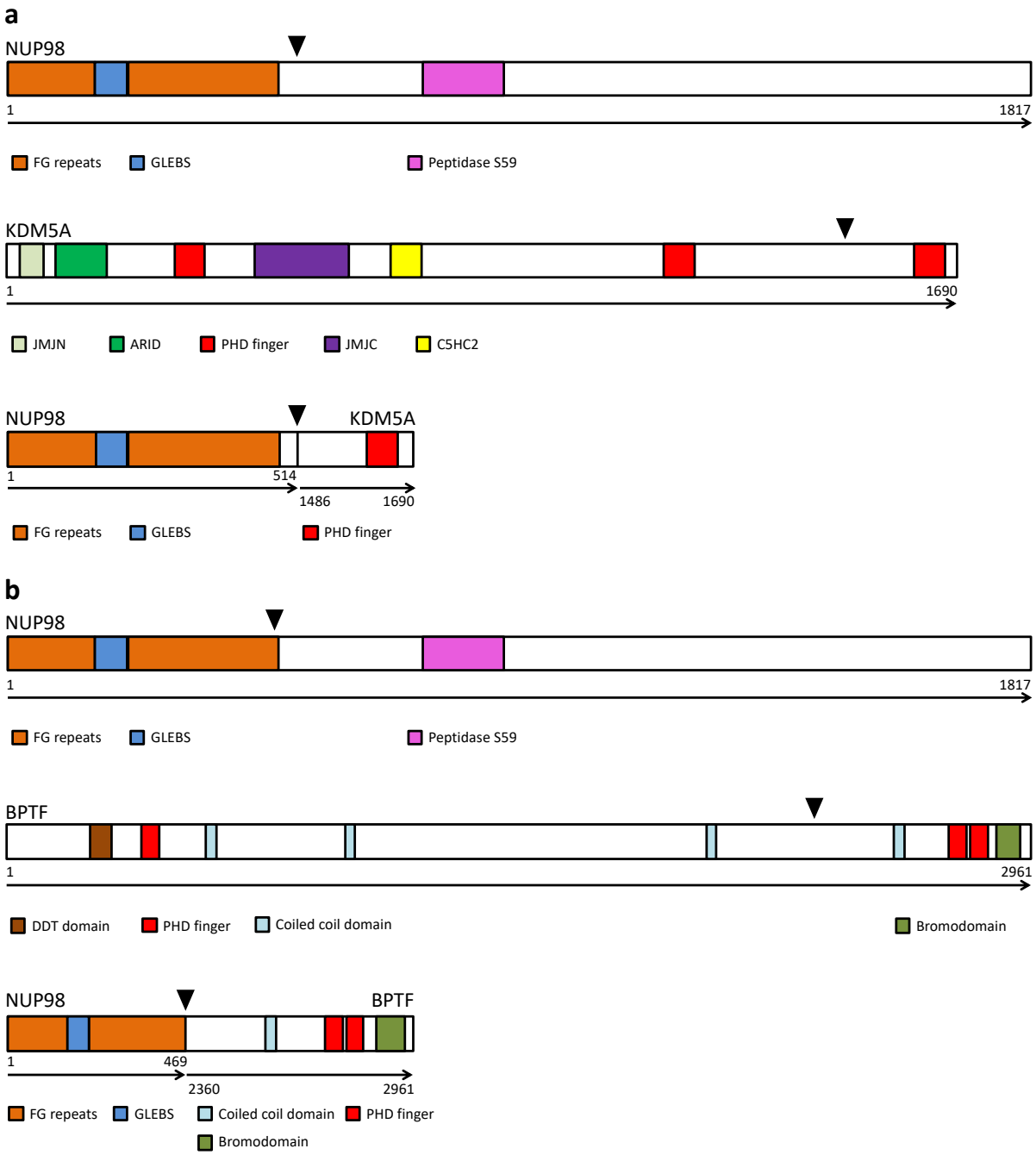

Supplementary Figure 3. Domain structures of proteins involved in **a** NUP98-KDM5A and **b** NUP98-BPTF fusions. Triangles represent fusion junctions. See Fig. 1d, h for legends.

Supplementary Table 1. Clinical data and additional summary of genomic findings from nine patients with adverse-risk AML

Case	Gender	Age	UHN Biobank ID	Diagnosis	Induction therapy	Primary refractory (Yes/No)	WGS coverage	# of chromosomal gains/losses		# of sub-chromosomal gains/losses		# of translocations/ inversions	
								Total	NGS concordant	Total	NGS concordant	Total	NGS concordant
1	M	55	0187	Secondary AML following MDS	3+7	No; died due to sepsis during induction	15.5	4	4	0	0	1	1
2	F	54	0619	AML (T/myeloid phenotype)	3+7	Yes	10.5	1	1	0	0	1	1
3	M	64	5726	AML	3+7 + lovostatin	Yes	14.9	7	2	20	6	4	1
4	F	42	8213	AML	3+7	No; died due to ICH during induction	10.1	3	3	0	0	3	2
5	M	33	8423	AML	3+7	Yes	9.6	0	0	2	1	2	2
6	F	20	8886	AML	3+7	Yes	11.6	1	1	1	1	1	1
7	M	46	080110	APL-like	3+7	Yes	11.2	6	3	0	0	2	2
8	F	64	522222	AML	3+7	Yes	6.5	6	1	4	2	4	3
9	F	70	130053	AML	3+7	Yes	11.9	0	0	0	0	1	1

	Chromosomal gains/losses	Sub-chromosomal gains/losses	Translocations/ inversions
Concordance rate	53.6%	37.0%	73.7%

Supplementary Table 2. List of bioinformatics tools used in this study and their references

Algorithm	Version	Purpose	Reference
BWA	0.7.4	Whole-genome sequencing alignment	Li H, Durbin R. Fast and accurate short read alignment with Burrows-Wheeler transform. Bioinformatics 2009; 25: 1754–1760.
CREST	1.0	Structural variant detection	Wang J, Mullighan CG, Easton J, Roberts S, Heatley SL, Ma J et al. CREST maps somatic structural variation in cancer genomes with base-pair resolution. Nat Methods 2011; 8: 652–654.
HMMcopy	0.1.1	Copy number analysis	Ha G, Roth A, Lai D, Bashashati A, Ding J, Goya R et al. Integrative analysis of genome-wide loss of heterozygosity and monoallelic expression at nucleotide resolution reveals disrupted pathways in triple-negative breast cancer. Genome Res 2012; 22: 1995–2007.
STAR	2.5.2a	RNA-seq alignment	Dobin A, Davis CA, Schlesinger F, Drenkow J, Zaleski C, Jha S et al. STAR: ultrafast universal RNA-seq aligner. Bioinformatics 2013; 29: 15–21.
STAR-Fusion	1.0.0	Fusion transcript detection	Haas B, Dobin A, Stransky N, Li B, Yang X, Tickle T et al. STAR-Fusion: Fast and Accurate Fusion Transcript Detection from RNA-Seq. bioRxiv (Preprint) 2017. doi:10.1101/120295.
GATK	3.6.0	SNV and indel calling	Poplin R, Ruano-Rubio V, DePristo MA, Fennell TJ, Carneiro MO, Van der Auwera GA et al. Scaling accurate genetic variant discovery to tens of thousands of samples. bioRxiv (Preprint) 2018. doi:10.1101/201178.
IGV	2.3.88	Visualization of sequencing data	Thorvaldsdottir H, Robinson JT, Mesirov JP. Integrative Genomics Viewer (IGV): high-performance genomics data visualization and exploration. Briefings in Bioinformatics 2013; 14: 178–192.

Supplementary Table 3. Individual cytogenetic abnormalities and concordant NGS findings

Case	Karyotype (NGS concordant abnormalities listed underneath)	NGS findings		
		Copy number gain	Copy number loss	Chromosomal rearrangement
1	51, XY, **+Y**, **+der(1;7)(q10;p10)**, **+6**, **+8**, **+10** [10]			
	+Y	**Y**		
	+der(1;7)(q10;p10)	**1q, 7p**		
	+6	**6**		
	+8	**8**		
	+10	**10**		
2	45, XX, **-7** [17] / 45, **X**, **t(X;8)(p21.2;q24.1)**, **-7** [2] / 46, XX[1]			
	-7		**7**	
	t(X;8)(p21.2;q24.1)		*BCOR*	**t(X;8)(p11.4;q24.13)** linked to *BCOR* deletion
3	43~45, **X**, **-Y**, t(1;5)(q21;p13), t(1;6)(q21;p25), -2, **add(2)(p21)**, **add(3)(q27)**, **del(3)(q27)**, add(4)(p16), del(4)(q33), del(5)(q31), add(6)(p25), del(6)(q21), -7, add(7)(q36), **del(7)(q22)**, -8, **add(8)(q24.3)**, del(8)(?q23), +del(8)(q22), add(9)(p22), add(9)(q34), add(11)(p15), **add(12)(p13)**, -16, add(16)(p13.3), **-17**, **der(17)t(11;17)(q13;p13)**, add(18)(q23), der(19)t(11;19)(q13;q13.3), -21, add(22)(p11.2), +4mar [cp20]			
	-Y		**Yq11.221-q12**	
	add(2)(p21)	**2p21-p11.2** (*BCL11A*)		
	add(3)(q27)	**3q26.32-q29**		
	del(3)(q27)			chr**2**/**3**/**8**/**11**/**12**/16/ **17**/19/X rearrangements
	del(7)(q22)		**7q21.3-q36.2**	
	add(8)(q24.3)	**8q12.1-q23.1** (*RUNX1T1*)		
	add(12)(p13)	**12p13.33-p13.2**		
	-17		**17p13.3-p12** (*TP53*), **17q11.2-q24.3** (*NF1*)	
	der(17)t(11;17)(q13;p13)	**11q13.4-q25** (*ETS1*)		chr**2**/**3**/**8**/**11**/**12**/16/ **17**/19/X rearrangements
4	48-49, XX, **+6**, **+8**, **+9**, **t(12;17)(p13;q11.2)**, i(17)(q10), **inv(18)(q11.2q21)** [cp20]			
	+6	**6**		
	+8	**8**		
	+9	**9**		
	t(12;17)(p13;q11.2)			t(11;**12**;**17**)(p15.4;**p13.3**; **q11.2**) linked to gene fusion
	inv(18)(q11.2q21)		**18q21.2** (*SMAD4*)	
5	46, XY, **del(6)(q21q23)**, **t(10;11)(p1?2;q21)**, **inv(12)(q15q24.1)**, del(15)(q2?4) [cp19] / 46, XY [1]			
	del(6)(q21q23)		**6q16.1-q22.31** (*FOXO3*)	
	t(10;11)(p1?2;q21)			**t(10;11)**(p12.3;q14.2) linked to gene fusion
	inv(12)(q15q24.1)			**chr12 rearrangements** linked to *SH2B3* and *TBX3* deletions
6	46, XX, **del(5)(q31)**, **t(11;12)(p13;p13)** [4] / 45, **idem**, **-13** [5] / 46, XX [1]			
	del(5)(q31)		**5q22.2q32** (*APC*)	
	t(11;12)(p13;p13)			chr**11**/**12**/17 rearrangements linked to CNVs and gene fusion (Figure 1)
	-13		**13**	

Case	Karyotype (NGS concordant abnormalities listed underneath)	NGS findings		
		Copy number gain	Copy number loss	Chromosomal rearrangement
7	43~48, XY, +?Y, +?Y, **der(5)t(5;17)(q1?3;q11.2)**, **-7**, **+8**, **-12**, -13, **t(16;18)(q24;q23)**, +1~2mar [cp10]			
	der(5)t(5;17)(q1?3;q11.2)			chr2/**5**/**12**/13/**16**/**17**/**18** rearrangements
	-7		**7**	
	+8	**8**		
	-12		**12p13.2-p12.1** (*ETV6*), **12p12.1-p11.21**, **12q12-q24.13**	chr2/**5**/**12**/13/**16**/**17**/**18** rearrangements
	t(16;18)(q24;q23)			chr2/**5**/**12**/13/**16**/**17**/**18** rearrangements
8	42-45, X, der(X)t(X;3)(q28;q21), **der(1)t(1;17)(p35;q21)**, **-3**, -5, **add(8)(q13)**, -9, add(11)(q13), add(12)(q24), **i(13)(q10)**, **del(16)(q23)**, -17, -18, -19, **+idic(22)(p12)**, +2r, +mar1 [cp9] / 46, XX [1]			
	der(1)t(1;17)(p35;q21)			chr**1**/5/**8**/9/11/12/**16**/**17**/19 rearrangements
	-3		**3**	
	add(8)(q13)	**8q** (*MYC*)		chr**1**/5/**8**/9/11/12/**16**/**17**/19 rearrangements
	i(13)(q10)	**13**		
	del(16)(q23)		**16q21-q24.3** (*CTCF*)	chr**1**/5/**8**/9/11/12/**16**/**17**/19 rearrangements
	+idic(22)(p12)	**22**		
9	46, XX, **t(1;14)(q21;q11.2)** [20]			
	t(1;14)(q21;q11.2)			**t(1;14)(q23.2;q12)** linked to truncation of *ATP1A2*

Supplementary Table 4. Cross-analysis of WGS and RNA-seq findings for gene fusion detection

Case	WGS									RNA-seq										Description	Driver gene fusion
	Left chr	Left pos	Left strand	Right chr	Right pos	Right strand	Left gene	Right gene	Gene orientation	Left chr	Left pos	Left strand	Right chr	Right pos	Right strand	Left gene	Right gene	Junction read #	Spanning fragment #		
2	chr3	17738725	-	chr15	34634338	+	TBC1D5	NOP10	Opposite	chr3	17783973	-	chr15	34640170	+	TBC1D5	NUTM1	28	109	Out-of-frame; 5' UTR of *TBC1D5*	
	chrX	40023570	-	chrX	39523885	+	BCOR													#3 in Supp. Fig. 1; linked to *BCOR-RNF139* below	
	chrX	39524250	+	chr8	125414839	+														#2 in Supp. Fig. 1; linked to *BCOR-RNF139* below	
										chrX	40036260	-	chr8	125498072	+	BCOR	RNF139	4	2	Out-of-frame; 5' UTR of *BCOR*	
3	chr20	45972885	-	chr9	132665158	-	ZMYND8	FNBP1	Same	chr20	45976600	-	chr9	132662826	-	ZMYND8	FNBP1	88	210	Out-of-frame	
	chr12	12012826	+	chr3	168875442	-	ETV6	MECOM	Same	chr12	12006495	+	chr3	168861620	-	ETV6	MECOM	18	75	Out-of-frame	Increased expression of *MECOM* from an alternative translation start site
	chr5	66263319	+	chr1	235611175	+	MAST4	TBCE	Same											Out-of-frame	
	chr16	57065493	+	chr19	2275316	-	NLRC5	C19orf35	Same											3' UTR of *C19orf35*	
	chr17	35936207	+	chr17	30854871	+	SYNRG	MYO1D	Same											Out-of-frame	
	chr7	138769597	-	chr7	139432554	-	HIPK2	ZC3HAV1	Same	chr7	138774370	-	chr7	139416814	-	ZC3HAV1	HIPK2	26	48	Out-of-frame	
	chr17	56794315	-	chr17	57090343	+	RAD51C	TRIM37	Same											Out-of-frame; *TRIM37* is massively rearranged	
	chr17	57018384	+	chr17	57102178	-	PPM1E	TRIM37	Same											Out-of-frame; *TRIM37* is massively rearranged	
	chr7	138565338	+	chr4	151196527	+	KIAA1549	LRBA	Same											In-frame; *LRBA* is massively rearranged; no fusion transcript	
										chr4	151814204	-	chr7	138768778	-	LRBA	ZC3HAV1	20	54	Out-of-frame	
										chr7	139313699	-	chr4	151719294	-	HIPK2	LRBA	18	62	Out-of-frame	
										chr7	139030367	+	chr4	151186964	-	LUC7L2	LRBA	7	43	Out-of-frame	
	chr16	80782	-	chr12	10531157	-	IL9RP3	KLRK1	Same	chr16	81799	-	chr12	10530834	-	IL9RP3	KLRK1	3	2	In-frame; *IL9RP3* is a pseudogene	
4	chr11	3753668	-	chr12	404641	+	NUP98	KDM5A	Same	chr11	3756421	-	chr12	402335	-	NUP98	KDM5A	44	78	In-frame	Yes
5	chr11	85680853	-	chr10	21888265	+	PICALM	MLLT10	Same	chr11	85685751	-	chr10	21901277	+	PICALM	MLLT10	62	51	In-frame	Yes
	chr10	21888246	+	chr11	85680578	-	MLLT10	PICALM	Same	chr10	21884369	+	chr11	85670103	-	MLLT10	PICALM	23	99	In-frame	
6	chr11	3759564	-	chr17	65941452	+	NUP98	BPTF	Same	chr11	3765739	-	chr17	65941525	+	NUP98	BPTF	28	22	In-frame	Yes
	chr17	65941478	+	chr11	3758816	-	BPTF	NUP98	Same	chr17	65940488	+	chr11	3756554	-	BPTF	NUP98	7	46	In-frame	
	chr6	108833664	+	chr6	108890015	+	LACE1	FOXO3	Same											In-frame; no fusion transcript; low expression of *LACE1*	
7	chr13	21382331	-	chr8	41470742	+	XPO4	AGPAT6	Same											Out-of-frame	
	chr16	68808494	+	chr12	111922848	-	CDH1	ATXN2	Same											In-frame; no fusion transcript; no expression of *CDH1*	
	chr17	36953437	+	chr17	36710058	+	PIP4K2B	SRCIN1	Same											Out-of-frame	
	chr1	22453096	+	chr1	28159637	-	WNT4	PPP1R8	Same											Out-of-frame	
	chr2	86740965	-	chr18	75954665	+	CHMP3													Linked to *CHMP3-CDH3* below	
	chr18	75966176	+	chr16	68756154	+		CDH3												Linked to *CHMP3-CDH3* below	
										chr2	86756341	-	chr16	68756328	+	CHMP3	CDH3	51	114	In-frame; putative alternative transcript of *CDH3*	
	chr7	157134847	+	chr7	71504707	-	CALN1	DNAJB6	Same	chr7	157129838	+	chr7	71488754	-	DNAJB6	CALN1	12	42	Inversion; out-of-frame; 5' UTR of *DNAJB6*	
8	chr9	115804777	+	chr1	19501815	+	ZFP37	UBR4	Same											3' UTR of *ZFP37*	
	chr8	40573882	-	chr12	27101439	+	ZMAT4	FGFR1OP2	Same											Out-of-frame; 5' UTR of *FGFR1OP2*	
	chr11	120815777	+	chr11	121009286	+	GRIK4	TECTA	Same											In-frame; no fusion transcript; no expression of both genes	
	chr16	89500468	-	chr17	28688888	+	ANKRD11			chr16	89556653	-	chr17	28712007	+	ANKRD11	CPD	3	3	Out-of-frame; 5' UTR of *ANKRD11*	

Supplementary Table 5. Literature review of three cases with *NUP98-BPTF* fusion

Case	1	2	3
Reference	Yasuda *et al*., 2016	Roussy *et al*., 2018	This study (#6)
Sex	Female	Male	Female
Age	19 years	8 months	20 years
Diagnosis	T-cell acute lymphoblastic leukemia	Acute megakaryoblastic leukemia	Acute myeloid leukemia
Karyotype	86~89, XXXX, +X, add(1)(p36), -4, -5, -6, ?add(6)(q21), -7, -8, -9, -10, -11, der(11)add(11)(p11) add(11)(q23), -13, -14, -15, -16, -17, -18, -18, -20, -21, +11, ~15mar, inc [cp5] / 46, XX [14]	49, XY, +6, +7, t(11;17)(p15;q23), +19	46, XX, del(5)(q31), t(11;12)(p13;p13) [4] / 45, idem, -13 [5] / 46, XX [1]
NUP98 exons	Not available	1-11	1-12
BPTF exons	Not available	26-30*	23-30*

NUP98 exons are derived from Refseq transcript NM_016320, and *BPTF* exons are derived from Refseq transcript NM_004459. *An additional 174-bp exon is included between exons 26 and 27 at chr17:65,959,449-65,959,622 (ref. 11).

Supplementary Table 6. Immunophenotype of case 5 at diagnosis and progression

	Diagnosis	Progression
Myelomonocytic associated markers		
CD11b	0.32	0.42
CD13	0.57	0.45
CD15	0.02	0.01
CD33	0.08	0.45
CD34	0.38	0.51
CD56	<0.01	0.02
CD65	0.03	0.01
CD117	0.01	0.30
HLA-DR	0.92	0.91
CD33+CD34+	0.06	0.40
Lymphoid markers		
CD2	0.04	0.03
CD3	0.01	<0.01
CD4+CD3+	<0.01	NA
CD4	NA	0.03
CD5	0.05	NA
CD7	>0.99	0.98
CD8+CD3+	<0.01	NA
CD10	0.01	<0.01
CD19	0.06	0.17
Intracellular markers		
TdT	0.01	0.01
MPO	<0.01	<0.01
CyCD3	0.01	0.02
CyCD79a	0.61	0.43
CyCD22	0.02	NA

Blasts are gated on CD45 versus side scatter. Blast region contains ~86% of gated cells at diagnosis and ~55% at relapse.